High-spin structure of ^{105}Ag: Search for chiral doublet bands

J. Timár,[1] T. Koike,[2,3] N. Pietralla,[2,4] G. Rainovski,[2,5] D. Sohler,[1] T. Ahn,[2,4] G. Berek,[1] A. Costin,[2,4] K. Dusling,[2] T. C. Li,[2] E. S. Paul,[6] K. Starosta,[7] and C. Vaman[2,7]

[1]*Institute of Nuclear Research, Pf. 51, H-4001 Debrecen, Hungary*

[2]*Department of Physics and Astronomy, SUNY, Stony Brook, New York 11794-3800, USA*

[3]*Graduate School of Science, Tohoku University, Sendai 980-8578, Japan*

[4]*Institut für Kernphysik, Technische Universität Darmstadt, D-64289 Darmstadt, Germany*

[5]*Faculty of Physics, St. Kliment Ohridski University of Sofia, BG-1164 Sofia, Bulgaria*

[6]*Oliver Lodge Laboratory, Department of Physics, University of Liverpool, Liverpool L69 7ZE, United Kingdom*

[7]*NSCL, Cyclotron Laboratory, Michigan State University, East Lansing, Michigan 48824-1321, USA*

(Received 11 April 2007; published 6 August 2007)

The high-spin structure of the ^{105}Ag nucleus has been studied by using the ^{100}Mo(^{10}B, $5n$)^{105}Ag reaction to search for chiral doublet bands based on the three-quasiparticle $\pi g_{9/2}\nu(h_{11/2})^2$ configuration. The level scheme of ^{105}Ag has been extended. New bands were found and the placement of the yrast $\pi g_{9/2}\nu(h_{11/2})^2$ band was corrected. No side band to the yrast $\pi g_{9/2}\nu(h_{11/2})^2$ band could be found in the present experiment. This observation indicates that the γ-soft shape in the ^{106}Ag changed to a more γ-rigid axially symmetric shape in the yrast ^{105}Ag configuration. However, a new pair of bands was observed to show the expected properties of a chiral doublet structure.

DOI: 10.1103/PhysRevC.76.024307 PACS number(s): 21.10.Re, 21.60.−n, 23.20.Lv, 27.60.+j

I. INTRODUCTION

The existence of nuclear chirality is one of the most intriguing questions of contemporary high-spin nuclear structure studies. Chiral rotation is generated when the total angular momentum vector of a rotating triaxial nucleus is out of the three symmetry planes of the triaxial mean field [1,2]. In this case the three projections of the angular momentum vector on the principal axes can form a right-handed or a left-handed system. This special direction of the angular momentum arises from the mutually perpendicular orientation of the core rotation and the angular momenta of the high-j valence particles and produces a linked pair of degenerate rotational bands. Rotational doublet-band candidates for chiral structures have been observed mostly in two regions of the nuclear chart: around ^{134}Pr (see, e.g., Refs. [3–16]) and around ^{104}Rh (see, e.g., Refs. [17–22]). In this second region the Rh isotopes are rather well studied. Besides these nuclides, only in ^{100}Tc has chiral doubling been proposed based on experimental data. Thus it is very interesting to study these doublet bands in the nearby Ag nuclei.

In the Rh/Ag/Tc region, chiral rotation is expected for the $\pi g_{9/2}\nu h_{11/2}$ configuration in odd-odd nuclei and for the $\pi g_{9/2}\nu(h_{11/2})^2$ configuration in odd-mass nuclei. Jerrestam *et al.* [23] reported rather intensive side bands to these configurations in ^{106}Ag and ^{107}Ag, respectively. The ^{106}Ag case was reinvestigated recently by Joshi *et al.* [24]. They suggested that the nature of the doublet band structure in this nucleus is quite different from the Rh cases. Though the quasiparticle configurations of both bands in the doublet in ^{106}Ag is $\pi g_{9/2}\nu h_{11/2}$, as in the odd-odd Rh cases, they belong to different shapes because of the γ-softness of the nucleus; the yrast is triaxial and the yrare is axially symmetric. The nature of the doublet structure in ^{106}Ag looks similar to the case of ^{134}Pr [25,26]. The $\pi g_{9/2}\nu h_{11/2}(g_{7/2}, d_{5/2})$ configuration can also result in chiral coupling of angular momenta in odd-mass triaxial nuclei (see Ref. [20]); however, because it is not a unique-parity configuration, it is very difficult to provide unique experimental observables confirming the nature of the doubling of states [21].

In Ref. [22] it has been shown that in the Rh nuclei the behavior of the two-quasiparticle $\pi g_{9/2}\nu h_{11/2}$ and the three-quasiparticle $\pi g_{9/2}\nu(h_{11/2})^2$ doublets belonging to the same even-even core are very similar, whereas the behavior of the doublets belonging to the neighboring even-even cores differs considerably. It is interesting to examine how the properties of the chiral candidate doublet structures evolve as a function of the neutron number in the Ag nuclei, that is, how the conditions of chiral geometry vary in the Ag isotope chain. The side band of the $\pi g_{9/2}\nu(h_{11/2})^2$ configuration band in ^{107}Ag (see Ref. [23]) seems to show similar properties (crossing of the bands, relative quasiparticle alignments, and relative kinematic moments of inertia) to the side band of the $\pi g_{9/2}\nu h_{11/2}$ band in ^{106}Ag, though its configuration assignment is not completely clear yet. This observation may indicate that the properties of the two- and three-quasiparticle doublet band structures corresponding to the same even-even core in the Ag nuclei also behave similarly, as was observed in the Rh nuclei. Further information can be provided by examining ^{104}Ag and ^{105}Ag nuclei. Jerrestam *et al.* studied ^{105}Ag [27]. They did not report, however, a doublet band $\pi g_{9/2}\nu(h_{11/2})^2$ structure in that nucleus.

In the present study we have performed an experiment to investigate the high-spin states of ^{105}Ag with a larger sensitivity than was reported in Ref. [27] to decide whether the side band exists but is populated with a small, ∼0.1 intensity ratio, similarly to the Rh cases, or whether the ratio is considerably smaller than in the Rh cases. Observation of doublet band structure similar to the doublet bands in the Rh nuclei would indicate that the shape of ^{105}Ag changed to more

γ-rigid triaxial, which allows the chiral vibration. However, if the ratio is much smaller, it indicates that the shape changed to more γ-rigid axially symmetric one.

II. EXPERIMENTAL METHODS AND RESULTS

High-spin states in ^{105}Ag were populated by using the ^{100}Mo(^{10}B, $5n$) reaction at beam energies of 58 and 64 MeV. The beam was provided by the Stony Brook tandem-injected superconducting LINAC and it impinged on a 1.3 mg/cm^2 thick enriched ^{100}Mo target on a 20 mg/cm^2 natural Pb backing foil. The emitted γ rays were detected by six Compton-suppressed hyperpure germanium (HPGe) detectors and a 14-element bismuth germanate (BGO) multiplicity filter. Approximately 10^8 $\gamma\gamma$ coincidence events were collected. The Ge detectors were calibrated for both energy and efficiency by using a ^{152}Eu source placed at the target position.

The directional correlations of oriented nuclei (DCO) ratios [28] were measured for transitions of sufficient intensity to determine their multipolarity. For the measurement, pairs of detectors were placed at forward, 90 degree, and backward directions. An asymmetric $\gamma\gamma$ matrix comprising γ rays detected by the forward and backward detectors along one axis and by detectors at 90 degrees along the other axis was created The ratios $R_{\rm DCO} = I_{\gamma\gamma}$ (forward + backward, 90°[gate])/$I_{\gamma\gamma}$(90°, forward + backward [gate]) were extracted. For this geometry $R_{\rm DCO} \approx 0.6$ is expected for a pure stretched dipole and $R_{\rm DCO} = 1$ for a stretched quadrupole transition when gating on a stretched quadrupole transition. When setting the gate on a pure stretched dipole transition, the expected $R_{\rm DCO}$ ratios are 1 and ≈1.5, respectively.

Typical γ-ray coincidence spectra are shown in Fig. 1. The derived γ-ray energies, relative intensities, and $R_{\rm DCO}$ ratios are listed in Table I.

A partial level scheme for ^{105}Ag derived from the present experiment is shown in Fig. 2. The level scheme was constructed on the basis of the measured $\gamma\gamma$ coincidence relations, as well as energy and intensity balances extracted for the observed γ rays with the use of the Radware analysis package [29]. The γ rays are arranged into several band structures in Fig. 2, labeled A–G, to facilitate the discussion.

The medium-spin level scheme of ^{105}Ag was previously studied by Hippe *et al.* [30], Rakesh Popli *et al.* [31], Kalshoven *et al.* [32], and Keller *et al.* [33]. The most complete medium-spin level scheme was derived by Keller *et al.* using the ^{103}Rh(α, $2n$) reaction. They observed band A up to spin 17/2, band B up to spin 21/2, as well as the dipole cascades of bands C and D up to spins 29/2 and 25/2, respectively. They assigned firm spin-parity values to the observed levels on the basis of the γ-ray angular distribution and the linear polarization measurement. Here these spin-parity assignments are followed for the low-energy levels whereas spin parities for selected higher energy levels are reassigned based on γ-ray multipolarities obtained from the present DCO measurements.

Jerrestam *et al.* [27] studied high-spin bands in ^{105}Ag using the ^{76}Ge(^{37}Cl, $\alpha 4n$) reaction. They observed band A up to spin 21/2, band C up to spin 39/2, and band E up to spin 41/2. However, as will be discussed in the following, they placed band E differently from its placement in Fig. 2, and consequently the spin parities of the levels suggested by them are also different. The spin parities suggested for the levels in bands A and C agree well with the ones reported by Keller *et al.* [33].

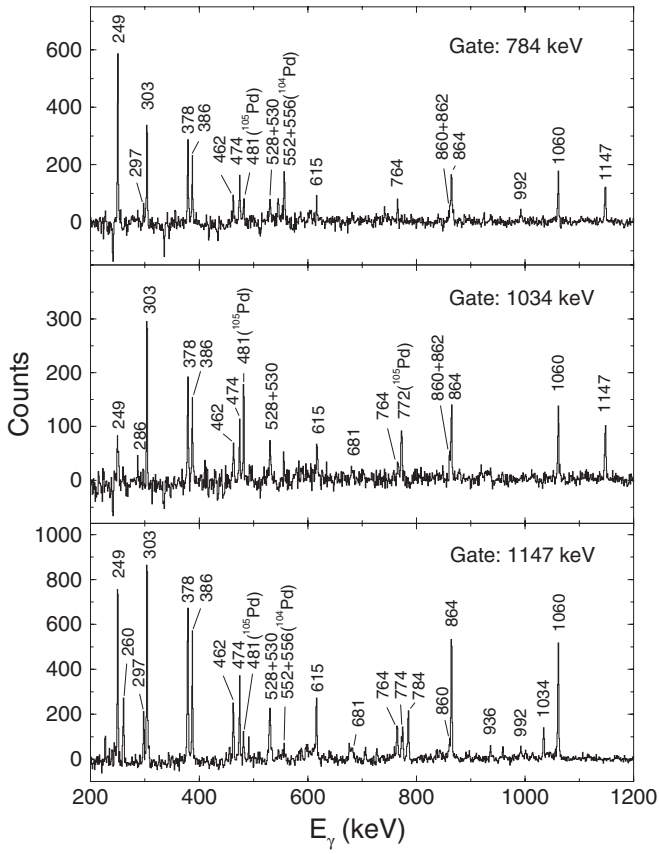

FIG. 1. Typical $\gamma\gamma$ coincidence spectra from the present experiment. The spectra show coincidence relationships that prove the new placement of band E.

Jerrestam *et al.* [34] have also observed a highly deformed band in ^{105}Ag that was not observed in the present work. It is probably far nonyrast in the presently observed spin region. Very recently, Deo *et al.* [35] measured the lifetimes of several levels in the high-spin bands C and E. They accepted the level scheme published in Ref. [27].

Data obtained from the present experiment enabled us to considerably verify, extend, and correct the previously published level schemes as discussed in the following.

Band A has been extended by two levels at $19/2^+$ and $23/2^+$. The other states observed for this band agree with Refs. [33] and [27].

No new levels were found in *band B* from this experiment; however, several new transitions were found linking bands A and B. The existence of these transitions further strengthens the placements and spin-parity assignments of the levels in band B, though they are not strong enough to extract the corresponding DCO information. The DCO ratios obtained for the intense transitions feeding levels of band B agree well with the spin-parity assignments suggested by Ref. [33].

TABLE I. Energies, relative intensities, DCO ratios, and multipolarities of γ rays assigned to ^{105}Ag in the present work, as well as the excitation energy, spin, parity, and corresponding band assignments for the initial state for the decay. The experimental errors of the energies and relative intensities for the strong and/or well-resolved transitions are in the order of 0.1 keV and 5%, respectively. For weak or compound lines the errors can rise up to 1 keV and 50%. For the angular correlation results, [d] denotes a dipole gate set in the DCO ratio determination.

E_γ (keV)	I_γ (rel.)	R_{DCO}	Multipolarity	E_i (keV)	J_i^π	Band$_i$
98.7	6.9			2596	17/2−	C
125.8	8.3	0.49(6)	$M1+E2$	2596	17/2−	C
152.9	2.4	0.95(14)[d]	$M1$	2775	17/2−	D
155.5	41.6	0.56(6)	$M1+E2$	2751	19/2−	C
168.9	9.9	0.63(6)	$M1+E2$	2944	19/2−	D
184.7	40.3	0.62(7)	$M1+E2$	2936	21/2−	C
193.8	5.4	0.94(19)[d]	D	3102	(21/2−)	G
233.3	9.7	0.52(6)	$M1+E2$	3177	21/2−	D
240.2	38.2	0.52(5)	$M1+E2$	3176	23/2−	C
248.6	29.2	0.71(8)[d]	$M1+E2$	917	13/2+	A
249.0	8.1	0.49(6)	$M1+E2$	4159	25/2+	E
259.6	5.9	0.47(6)	$M1+E2$	4159	25/2+	E
285.7	0.8			3125	21/2+	A
290.4	4.2	0.31(7)	$M1+E2$	2313	19/2+	B
296.8	4.2	0.72(12)	$M1+E2$	1978	17/2+	A
297.0	8.3			2596	17/2−	C
303.0	17.6	0.49(6)	$M1+E2$	4462	27/2+	E
304.1	1.4			3786	(25/2−)	G
304.5	9.6	1.02(8)[d]	$M1+E2$	3482	(23/2−)	D
304.7	1.4			2775	17/2−	D
306.9	7.9	0.75(9)[d]	$M1+E2$	3409	(23/2−)	G
324.2	0.1			5856	(33/2−)	F
334.5	32.6	0.57(6)	$M1+E2$	3511	25/2−	C
334.8	0.7			2313	19/2+	B
341.4	3.5			2022	17/2+	B
350.3	5.1	0.54(9)	$M1+E2$	3102	(21/2−)	G
365.0	0.6			6221	(35/2−)	F
377.3	5.4	0.87(17)[d]	$M1+E2$	3786	(25/2−)	G
378.2	16.7	0.52(6)	$M1+E2$	4840	29/2+	E
379.9	2.5			3482	(23/2−)	D
385.5	5.0	0.81(17)[d]	$M1+E2$	3867	(25/2−)	D
386.3	16.0	0.50(6)	$M1+E2$	5226	31/2+	E
388.3	1.4			6609	(37/2−)	F
404.7	0.8			4718	(29/2−)	G
417.2	22.2	0.60(5)	$M1+E2$	3928	27/2−	C
424.8	1.5			3176	23/2−	C
430.5	1.0			5227	(31/2−)	G
433.9	18.3	0.52(9)	$M1+E2$	4362	29/2−	C
441.6	1.1			7051	(39/2−)	F
446.6	4.3	1.11(31)[d]	$M1+E2$	4314	(27/2−)	D
448.6	9.7	0.67(17)	$M1+E2$	2761	21/2+	B
452.3	1.4	1.04(25)[d]	$M1+E2$	2751	19/2−	C
462.0	7.6	0.48(5)	$M1+E2$	6162	35/2+	E
464.0	4.2	0.93(30)[d]	$M1+E2$	4250	(27/2−)	G
468.6	2.9			4718	(29/2−)	G
473.5	9.7	0.47(8)	$M1+E2$	5700	33/2+	E
483.0	2.4			4797	(29/2−)	D
508.5	1.5			5227	(31/2−)	G
513.3	6.4	0.52(9)	$M1+E2$	5445	33/2−	C
515.2	0.7			7566	(41/2−)	F
528.2	4.9	0.46(9)	$M1+E2$	7219	39/2+	E

TABLE I. *(Continued.)*

E_γ (keV)	I_γ (rel.)	R_{DCO}	Multipolarity	E_i (keV)	J_i^π	Band$_i$
529.6	6.9	0.46(9)	$M1+E2$	6691	37/2+	E
538.0	0.7			5335	(31/2−)	D
547.7	0.6			3899	23/2+	A
552.4	1.4			4462	27/2+	E
558.0	0.8			3909	23/2+	E
565.0	12.5	0.56(8)	$M1+E2$	2299	17/2−	
570.1	9.4	0.60(8)	$M1+E2$	4932	31/2−	C
574.7	2.4	1.12(26)	$E2$	3511	25/2−	C
579.1	11.8	1.06(23)	$E2$	2313	19/2+	B
586.2	1.7			7806	41/2+	E
603.5	1.7			6717	37/2−	C
609.1	2.2	1.01(15)[d]	D	2908	(19/2−)	G
615.3	60.4	0.74(11)	$M1+E2$	669	11/2+	A
668.4	2.9			6114	35/2−	C
681.3	2.5	0.93(16)	$E2$	4840	29/2+	E
689.0	0.1			6221	(35/2−)	F
690.1	0.6			3867	(25/2−)	D
739.1	1.3	1.08(26)	$E2$	2761	21/2+	B
752.0	3.2	1.73(32)[d]	$E2$	3928	27/2−	C
753.6	0.2			6609	(37/2−)	F
763.8	26.4	0.70(8)	$M1+E2$	1681	15/2+	A
764.0	2.5			5226	31/2+	E
773.9	2.8	0.56(15)	$M1+E2$	3899	23/2+	A
784.3	4.4	0.54(9)	$M1+E2$	3909	23/2+	E
796.9	1.9			2775	17/2−	D
807.2	0.8			4159	25/2+	E
816.4	8.7	0.43(6)	$M1+E2$	1734	15/2+	B
830.4	0.3			7051	(39/2−)	F
832.2	1.2			4314	(27/2−)	D
841.2	1.5			4250	(27/2−)	G
851.3	5.1	1.02(19)	$E2$	4362	29/2−	C
860.0	2.8	1.79(25)[d]	$E2$	5700	33/2+	E
861.5	7.6			2839	19/2+	A
864.1	100.0	1.08(10)	$E2$	917	13/2+	A
885.6	1.3			2908	(19/2−)	G
912.2	0.6			4840	29/2+	E
914.9	9.7	0.54(8)	$E1$	2596	17/2−	C
929.3	0.8			4797	(29/2−)	D
930.3	2.3			2908	(19/2−)	G
932.3	0.9			4718	(29/2−)	G
935.6	2.9	0.94(17)	$E2$	6162	35/2+	E
940.9	2.9			2622	(15/2−)	D
951.3	0.6			4462	27/2+	E
958.0	0.4			7566	(41/2−)	F
977.5	1.1			5227	(31/2−)	G
982.5	1.2	0.97(17)[d]	$E1$	4159	25/2+	E
991.7	1.7			6691	37/2+	E
1004.0	2.2	1.74(29)[d]	$E2$	4932	31/2−	C
1012.4	10.4	1.97(40)[d]	$E2$	1681	15/2+	A
1020.8	0.4			5335	(31/2−)	D
1033.5	3.9	1.11(23)	$E2$	4159	25/2+	E
1057.5	1.4			7219	39/2+	E
1059.7	4.2			3899	23/2+	A
1060.5	30.6	1.00(9)	$E2$	1978	17/2+	A
1065.0	20.1	1.75(19)[d]	$E2$	1734	15/2+	B
1070.0	2.8	1.78(39)[d]	$E2$	3909	23/2+	E
1083.4	3.5	1.69(31)[d]	$E2$	5445	33/2−	C

TABLE I. *(Continued.)*

E_γ (keV)	I_γ (rel.)	R_{DCO}	Multipolarity	E_i (keV)	J_i^π	Band$_i$
1093.7	4.3	0.57(17)	D	2775	17/2−	D
1102.5	1.4			3125	21/2+	A
1105.2	13.9	0.99(12)	*E*2	2022	17/2+	B
1114.3	0.6			7806	41/2+	E
1137.6	1.3			3899	23/2+	A
1147.1	12.5	1.05(19)	*E*2	3125	21/2+	A
1158.3	3.5			2839	19/2+	A
1163.5	0.9			6609	(37/2−)	F
1182.0	1.1			6114	35/2−	C
1272.1	1.2			6717	37/2−	C
1288.8	1.2			6221	(35/2−)	F
1373.5	2.6			3351	21/2+	
1493.8	1.4			5856	(33/2−)	F
1552.9	16.7	0.48(7)	*E*1	2470	15/2−	C
1580.1	25.6	0.49(6)	*E*1	2497	15/2−	C
1603.4	0.6			5531	(31/2−)	F

Band C and its linking transitions to the lower energy levels obtained from the present experiment are the same as published by Jerrestam *et al*. except that the highest energy 39/2$^-$ level was unobserved. The DCO ratios derived from the present experiment agree well with the spin-parity assignments of Refs. [33] and [27].

Both the placement of the transitions and the assigned spin parities of the lower energy part of *band D* in Fig. 2 agree well

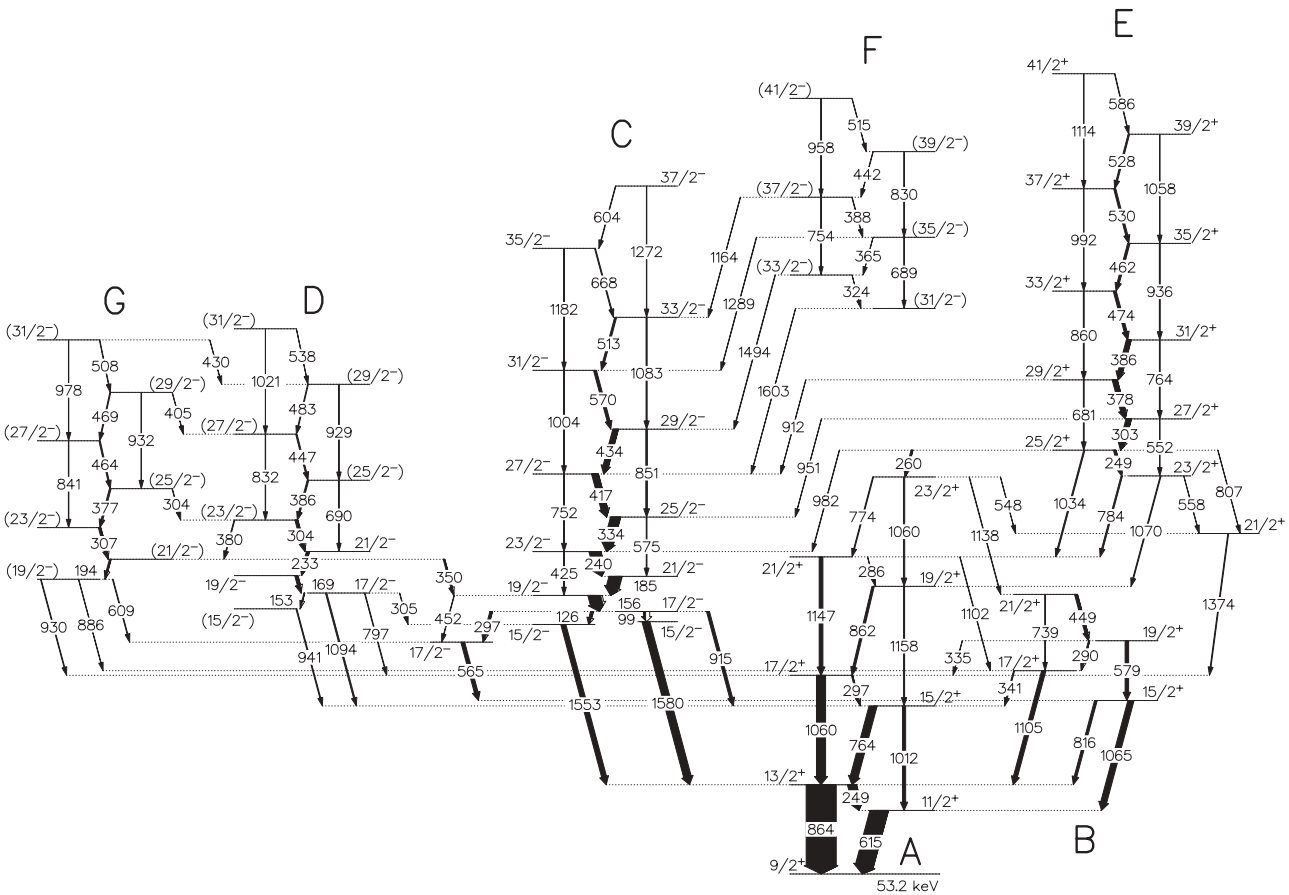

FIG. 2. Partial level scheme of ^{105}Ag obtained in the present work. The energies are given in keV; the width of the transitions are proportional to their relative intensities.

with the dipole band structure reported by Keller *et al.* [33]. From the present data this band could be extended by three higher energy levels, up to spin 31/2. The tentative spin-parity assignments of the highest energy levels are based on the spin parities of the lower energy part and on the dipole-cascade plus crossover structure of the band, where the dipoles are assumed to be $M1$ transitions and the crossovers to be of the $E2$ multipolarity.

Band E was also observed by Jerrestam *et al.* However, they did not observe the relatively weak linking transitions to bands A and C; therefore they assumed that the strong 303-keV dipole transition in band E feeds the $21/2^+$ state of band A directly. Their spin-parity assignments for the levels in band E were based on this assumption and on the measured DCO ratios. As a result of the present experiment, many weaker transitions were found between bands E and A, as well as between bands E and C, which modify the placement of band E and the spin-parity assignments for the levels in the band. To illustrate the $\gamma\gamma$ coincidence relations between the new transitions and the transitions in bands E and A, we plotted in Fig. 1 the coincidence spectra of the 784- and the 1034-keV γ rays. The measured DCO ratios of the strongest linking transitions made it possible to determine the spins and parities of the levels in band E. The state that is fed by the strong 303-keV transition decays by the stretched quadrupole 1034-keV γ ray to the $21/2^+$ state of band A, by the stretched dipole 982-keV γ ray to the $23/2^-$ state of band C, and also by the stretched dipole 260-keV γ ray to the $23/2^+$ state of band A. These decays imply that the spin of the depopulating level is 25/2. If the parity of this state is positive then the 982-keV dipole transition and the 1034-keV quadrupole transition are $E1$ and $E2$, respectively, whereas if the parity is negative then the $M1$ and $M2$ multipolarities should be observed, respectively. The relative intensity of the 1034-keV transition is larger than that of the 982-keV transition. This fact is in a good agreement with the $E1$ and $E2$ multipolarity assignments but in disagreement with the $M1$ and $M2$ assignments because of the strength of an $M2$ transition is expected to be about six orders of magnitude less than an $M1$ transition for the observed γ-ray energies. This argument suggests positive parity for the level fed by the 303-keV transition. When reiterated for the stretched dipole transitions between the successive levels and the stretched quadrupole crossover transitions in band E the argument leads to the spin-parity assignments for states in band E as shown in Fig. 2. The decay of the $23/2^+$ state of band E to the $21/2^+$ and $19/2^+$ states of band A further supports these spin-parity assignments.

Band F was observed for the first time in the present experiment. It is linked by four high-energy transitions to band C. These transitions are rather weak. Therefore no DCO ratios could be derived for multipolarity assignments. As this band is observed to decay only to the negative-parity band C and no decay is seen to the positive-parity band E, the negative-parity assignment for this band is more probable. In this case the linking transitions can have $M1$ or $E2$ multipolarities. For bands of the same parity high-energy $E2$ transitions dominate the $M1$ links, which implies the tentative spin and parity assignments proposed for band F in Fig. 2.

Band G was also not observed before the present experiment. The spin assignments of the levels in this band are based on the stretched dipole character of the 350-keV transition to the $19/2^-$ state of band C and on the measured DCO ratios for the dipole cascade in the band. The tentative negative parity is very probable since there are several linking transitions between bands G and D.

III. DISCUSSION

The main aim of the present work was to search for a chiral partner band to the known $\pi g_{9/2}\nu(h_{11/2})^2$ band in ^{105}Ag (band E in this work). However, during the analysis of the obtained experimental data it turned out that the position of this band in the level scheme and its links to the lower energy levels do not agree with previously published results. This fact makes the previous spin-parity assignment and thus the configuration assignment, too, questionable. Thus, in the following, the configuration assignments for all the observed band structures are reinvestigated before the search for the possible chiral partner band is reported.

A. Configurations of the observed bands

To discuss the configurations of the observed bands, their experimental Routhians (E') and aligned angular momenta (I_x) were extracted as defined in Ref. [36] and compared to the total Routhian surface (TRS) calculations based on the Woods-Saxon cranking formalism [37–39]. The labeling of the TRS orbitals is given in Table II. The compared values are plotted in Figs. 3 and 4 for the positive- and negative-parity bands, respectively. The Routhians are normalized by adding the same constant value to all the experimental configurations in a way that the predicted and experimental values for band A are consistent.

To further strengthen the assignment of quasiparticle configurations for the observed bands, experimental $B(M1; I \rightarrow I-1)/B(E2; I \rightarrow I-2)$ ratios of reduced transition probabilities have been extracted from the measured $I_\gamma(M1)/I_\gamma(E2)$ branching ratios and compared with predictions obtained using the geometrical model of Dönau and Frauendorf [40]. In the calculations K_n and i_n were approximated with constant

TABLE II. Labels used for the quasineutron (n) and quasiproton (p) states of parity π and signature α; n denotes the nth state for a given set of the (π, α) quantum numbers.

$(\pi,\alpha)_n$	n Label	Shell model	$(\pi,\alpha)_n$	p Label	Shell model
$(+,+1/2)_1$	A	$d_{5/2}, g_{7/2}$	$(+,+1/2)_1$	a	$g_{9/2}$
$(+,-1/2)_1$	B	$d_{5/2}, g_{7/2}$	$(+,-1/2)_1$	b	$g_{9/2}$
$(+,+1/2)_2$	C	$d_{5/2}, g_{7/2}$	$(+,+1/2)_2$	c	$g_{9/2}$
$(+,-1/2)_2$	D	$d_{5/2}, g_{7/2}$	$(+,-1/2)_2$	d	$g_{9/2}$
$(-,-1/2)_1$	E	$h_{11/2}$			
$(-,+1/2)_1$	F	$h_{11/2}$			
$(-,-1/2)_2$	G	$h_{11/2}$			
$(-,+1/2)_2$	H	$h_{11/2}$			

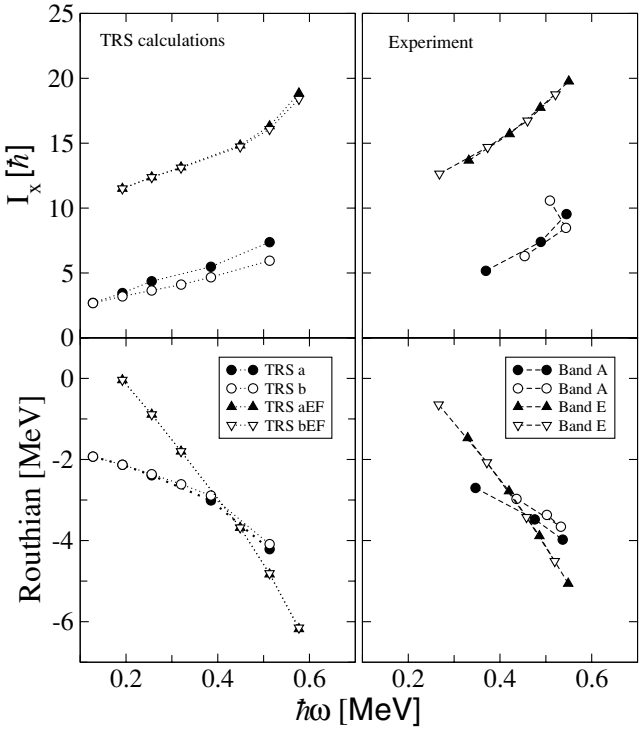

FIG. 3. Comparison between the experimental Routhians/aligned angular momenta and the TRS predictions for positive-parity bands.

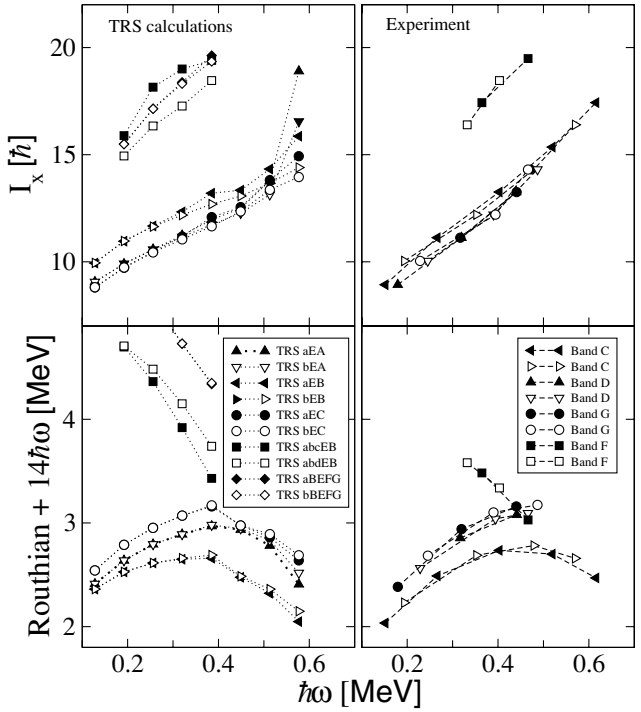

FIG. 4. Comparison between the experimental Routhians/aligned angular momenta and the TRS predictions for negative-parity bands.

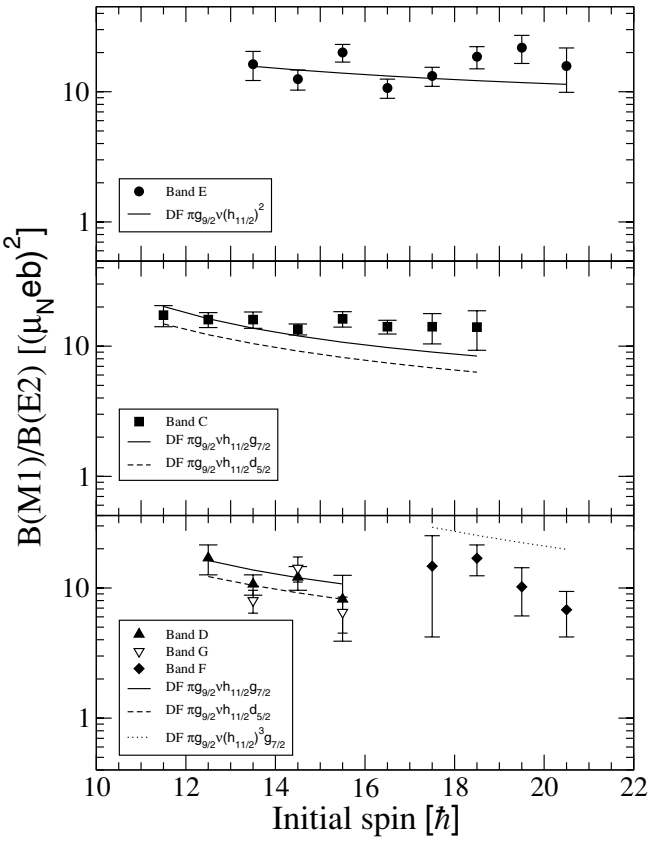

FIG. 5. Comparison between the experimental $B(M1; I \rightarrow I-1)/B(E2; I \rightarrow I-2)$ ratios and predictions obtained using the geometrical model of Dönau and Frauendorf.

values as listed in Table III; the appropriate g_n values were taken from Ref. [41]. The rotational gyromagnetic factor of $g_R = Z/A$ was used in the calculations, and the Q_0 electric quadrupole moments and the γ-shape parameters were derived from the nuclear shape predicted by the TRS calculations. The comparison is shown in Fig. 5.

1. The positive-parity bands

In the present experiment bands A, B, and E were assigned positive parity. Band A was previously reported in Refs. [27,33] with the $\pi g_{9/2}$ configuration assigned. Band B was reported by Keller *et al.* [33] but no firm configuration assignment could be made at that time. They suggested that levels in band B might correspond to $\pi g_{9/2}\nu(d_{5/2})^2$ or $\pi g_{9/2}\nu(g_{7/2}d_{5/2})$ configurations with a spherical shape. No

TABLE III. Parameters used to calculate $B(M1)/B(E2)$ ratios.

Configuration	g factor	K value	i_x
$\nu h_{11/2}$	−0.19	0.5	5.0
$\nu d_{5/2}$	−0.26	1.5	2.0
$\nu g_{7/2}$	+0.17	2.5	2.0
$\pi g_{9/2}$	+1.10	3.5	2.5

new information relevant to the configuration assignment of band B could be deduced from the present experiment.

Band E was reported previously in Ref. [27] with the $\pi g_{9/2}\nu(h_{11/2})^2$ configuration assignment. Though the parity of the band remained positive in the present analysis, the spins of the band members and thus the aligned angular momenta have been increased by $2\hbar$. This modification has a direct impact on the experimental Routhians.

In Fig. 3 the experimental Routhians and aligned angular momenta for bands A and E are plotted together with the Routhians and aligned angular momenta predicted by the TRS calculations for the lowest energy one-quasiparticle and three-quasiparticle positive-parity configurations. There is a rather good agreement between the experimental and predicted slopes and crossing frequencies of the Routhians, as well as between the experimental and predicted aligned angular momenta. On the basis of this agreement we can assign the a and b TRS configuration to the two signature branches of band A, and similarly the aEF and bEF TRS configurations to band E. These assignments confirm the previous $\pi g_{9/2}$ and $\pi g_{9/2}\nu(h_{11/2})^2$ configurations for bands A and E, respectively, and are not impacted by the new spin values extracted for band E or its new position in the level scheme. The configuration proposed for band E is further supported by the good agreement between the experimental and calculated $B(M1)/B(E2)$ ratios as seen in Fig. 5.

2. *The negative-parity bands*

The observed or tentative negative-parity bands are bands C, D, F, and G. Band C was previously reported in Refs. [27,33] and assigned the $\pi g_{9/2}\nu h_{11/2}(g_{7/2}, d_{5/2})$ configuration. The lower energy dipole cascade of band D was also reported in Ref. [33] and assigned as the second lowest energy band based on this configuration. Bands F and G were not reported previously.

The configuration assignments for bands C and D are confirmed by the present results. Experimental Routhians and aligned angular momenta of the negative-parity bands are compared to the TRS predictions for the three lowest energy three-quasiparticle configurations and for the two lowest energy five-quasiparticle configurations in Fig. 4. All three predicted lowest energy TRS configurations [i.e., (a,b)EB, (a,b)EA, and (a,b)EC] correspond to the $\pi g_{9/2}\nu h_{11/2}(g_{7/2}, d_{5/2})$ single-particle configurations. The good agreement between the experimental and calculated values show that bands C, D, and G are good candidates for the (a,b)EB, (a,b)EA, and (a,b)EC configurations, respectively. The deduced experimental $B(M1)/B(E2)$ ratios also support these assignments. It is worth noting that the bottom part of band E decays to band C via $E1$ transitions, for which the $B(E1)/B(E2)$ values could be deduced from the data. Assuming $Q_0 = 2\ e$ b for the quadrupole moment of band E, which is in agreement with the deformation predicted by the TRS calculations, we obtain $B(E1) \approx 2 \times 10^{-5}$ W.u. for these transitions. This $B(E1)$ value is not large enough to conclude octupole correlations. However, it is in agreement with the fact that the only difference between the two configurations is that one of the three quasiparticles occupies the $\nu h_{11/2}$ single-particle orbital in band E whereas it occupies the $\nu(g_{7/2}, d_{5/2})$ single-particle orbital in band C. This observation further supports the suggested configurations.

The aligned angular momenta for band F are larger than that of the other negative-parity bands by about $5\hbar$. Such large I_x values are predicted for five-quasiparticle configurations in this region, as shown in Fig. 4. Among the two plotted five-quasiparticle configurations in Fig. 4, abcEB,abdEB has the lower energy. However, this configuration is predicted to have quite a large signature splitting as compared to that observed for band F, whereas the signature splitting for the aBEFG,bBEFG configuration is predicted to be very small, in accordance with the experimental one. The calculated $B(M1)/B(E2)$ ratios for this latter configuration are close to the experimental values, but the calculated ratios for the abcEB,abdEB configuration are about two orders of magnitude too small (not plotted in Fig. 5). On the basis of these arguments the aBEFG,bBEFG configuration assignment for band F is more likely than the abcEB,abdEB. It should be stressed, however, that this configuration assignment is tentative. One should also note that no five-quasiparticle bands are reported in the neighboring Ag isotopes to compare with band F.

B. Comments on the existence of chirality in ^{105}Ag

The main aim of this study was to find a side band to the $\pi g_{9/2}\nu(h_{11/2})^2$ band in ^{105}Ag, which is band E in Fig. 2, and to determine the energy difference between the partners. The sensitivity of the current experiment and analysis is good enough to observe such a band if its population intensity was larger than one tenth of the population intensity of Band E. With this sensitivity no side band decaying to band E is detected.

According to the present result either there is no side band in ^{105}Ag or the energy difference between the side band and the $\pi g_{9/2}\nu(h_{11/2})^2$ band is considerably larger than in the cases of $^{102-106}$Rh. However, if the energy difference is very large then the chiral interpretation does not hold. Thus, we report here that there is no chiral partner band to the $\pi g_{9/2}\nu(h_{11/2})^2$ band in ^{105}Ag. This observation indicates that the γ-soft shape in ^{106}Ag changed to a more γ-rigid axially symmetric shape in ^{105}Ag. This is in agreement with the predictions of the present TRS calculations, and also with the results of the tilted axis cranking (TAC) calculations reported in Ref. [35].

It is interesting to compare the $\pi g_{9/2}\nu h_{11/2}(g_{7/2}, d_{5/2})$ bands in ^{105}Ag and in ^{105}Rh. In ^{105}Rh the second and third lowest energy bands of this configuration were reported as candidates for chiral partner bands based on the very small energy difference between the corresponding states, observation of strong linking transitions, and theoretical predictions by TAC calculations [20]. In ^{105}Ag bands D and G behave similarly. They are linked to each other by relatively strong transitions. In Fig. 6 we plotted the excitation energies, the $S(I) = [E(I) - E(I-1)]/2I$ energy-staggering values, as well as the $B(M1)/B(E2)$ ratios of the two bands. According

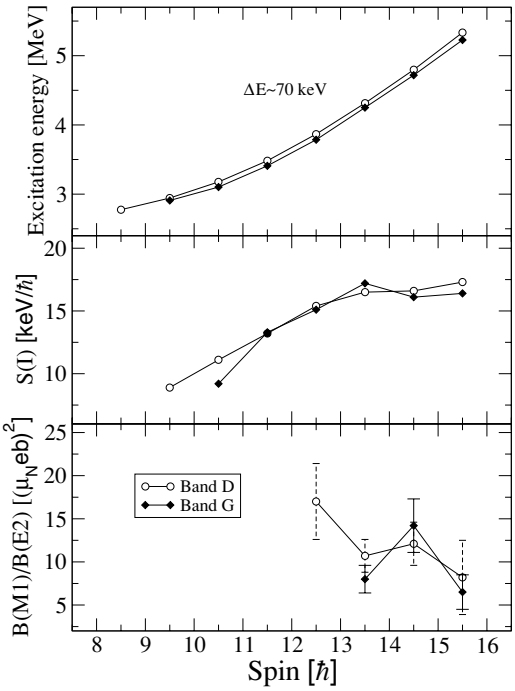

FIG. 6. Excitation energies, $S(I)$ values, and $B(M1)/B(E2)$ ratios of the bands D and G as a function of spin.

to the figure, the D and G band structure fulfills the criteria suggested for chiral candidate bands by Koike *et al.* [42].

(i) The energy difference is very small (≈70 keV) in the whole observed spin region. It is remarkable because no such small energy differences were found in such a wide spin range in chiral candidate doublets up to now.
(ii) The $S(I)$ energy-staggering curves are rather smooth. This is in agreement with the expectations for chiral rotation where the core rotation and the valence particle angular momenta are perpendicular to each other, resulting in small Coriolis interaction and diminished energy staggering of levels with consecutive spin.
(iii) The experimental $B(M1)/B(E2)$ ratios of the two bands agree within the experimental errors. Moreover, there is a pronounced staggering in the $B(M1)/B(E2)$ ratio values, whereas the $S(I)$ energy-staggering curves are smooth.

Though no TAC calculations were performed for these bands, their chiral behavior can be suggested based on the experimental results. Also, the results of the TAC calculations reported in Ref. [35] predicted a triaxial shape for band C, which has the same quasiparticle configuration as bands D and G. However, these results are not sufficient to prove the chiral behavior uniquely. The comparison of the derived experimental features of bands D and G with the results of TRS calculations and with general conciderations on chirality in three-quasiparticle cases does not allow us to distinguish the scenarios of chiral geometry and of simple mixing between the $\pi g_{9/2}\nu h_{11/2}(g_{7/2})$ and $\pi g_{9/2}\nu h_{11/2}(d_{5/2})$ configurations. Detailed quasiparticle-rotor model calculations capable of handling the chiral doubling in these three-quasiparticle configurations could provide specific differences between the two scenarios. Thus these results indicate a need for developing such a model.

If the D and G band structure results from formation of chirality, they represent the very stable chiral geometry over a wide spin range. However, the degeneracy is not perfect, and the $S(I)$ energy-staggering function is not completely smooth at the highest observed spins (Fig. 6). Therefore, this structure does not reflect a perfect chiral geometry, but it is a good candidate (together with other such band structures) for investigating what prevents these bands from being an ideal case. Thus studying these cases could also be an interesting direction of research.

IV. SUMMARY

The high-spin structure of the ^{105}Ag nucleus was studied by using the ^{100}Mo(^{10}B, $5n$)^{105}Ag reaction to search for chiral doublet bands with the three-quasiparticle $\pi g_{9/2}\nu(h_{11/2})^2$ configuration. The level scheme of ^{105}Ag has been extended. New bands were found and the placement of the yrast $\pi g_{9/2}\nu(h_{11/2})^2$ band was corrected. Experimental Routhians, aligned angular momenta, and $B(M1)/B(E2)$ ratios were derived from the data and compared with predictions of total Routhian surface calculations, as well as results of the geometrical model of Dönau and Frauendorf, respectively. On the basis of these comparisons configurations were assigned to the observed bands.

No side band to the yrast $\pi g_{9/2}\nu(h_{11/2})^2$ band could be found in the present experiment. This observation indicates that the γ-soft shape in ^{106}Ag changed to a more γ-rigid axially symmetric shape in the yrast ^{105}Ag configuration. However, the observation that the band structure D and G shows the properties of chiral doublet bands may indicate the presence of chirality in this nucleus. Nonetheless, since bands D and G are of natural parity, the observed similarities may be expected from excitations that do not involve chiral coupling of angular momenta.

It would be clearly interesting to examine the existence and the properties of similar side bands in the ^{108,109}Ag nuclei to find out how the nuclear shape changes on the higher mass side of ^{106,107}Ag, and if there are chiral Ag isotopes or if Ag is the high-Z border of the chiral mass ∼104 region.

ACKNOWLEDGMENTS

J. T. thanks the Department of Physics and Astronomy, SUNY, Stony Brook, for hospitality. The authors are indebted to A. Lipski for preparing the targets and to the accelerator staff for providing good-quality beams. This work was supported in part by the Hungarian Scientific Research Fund, OTKA (Contract No. T046901), the NAS under the COBASE program supported by Contract No. INT-0002341 from the NSF, and the U.S. National Science Foundation Grant No. PHY-0245018. G. R. acknowledges the support from the Bulgarian NSF under Contract No. VUF06/05.

[1] S. Frauendorf and J. Meng, Nucl. Phys. **A617**, 131 (1997).
[2] V. I. Dimitrov, S. Frauendorf, and F. Dönau, Phys. Rev. Lett. **84**, 5732 (2000).
[3] C. M. Petrache, D. Bazzacco, S. Lunardi, C. Rossi Alvarez, G. de Angelis, M. De Poli, D. Bucurescu, C. A. Ur, P. B. Semmes, and R. Wyss, Nucl. Phys. **A597**, 106 (1997).
[4] K. Starosta, T. Koike, C. J. Chiara, D. B. Fossan, D. R. LaFosse, A. A. Hecht, C. W. Beausang, M. A. Caprio, J. R. Cooper, R. Krücken, J. R. Novak, N. V. Zamfir, K. E. Zyromski, D. J. Hartley, D. L. Balabanski, J.-Y. Zhang, S. Frauendorf, and V. I. Dimitrov, Phys. Rev. Lett. **86**, 971 (2001).
[5] A. A. Hecht, C. W. Beausang, K. E. Zyromski, D. L. Balabanski, C. J. Barton, M. A. Caprio, R. F. Casten, J. R. Cooper, D. J. Hartley, R. Krücken, D. Meyer, H. Newman, J. R. Novak, E. S. Paul, N. Pietralla, A. Wolf, N. V. Zamfir, J.-Y. Zhang, and F. Dönau, Phys. Rev. C **63**, 051302(R) (2001).
[6] D. J. Hartley, L. L. Riedinger, M. A. Riley, D. L. Balabanski, F. G. Kondev, R. W. Laird, J. Pfohl, D. E. Archer, T. B. Brown, R. M. Clark, M. Devlin, P. Fallon, I. M. Hibbert, D. T. Joss, D. R. LaFosse, P. J. Nolan, N. J. O'Brien, E. S. Paul, D. G. Sarantites, R. K. Sheline, S. L. Shepherd, J. Simpson, R. Wadsworth, J.-Y. Zhang, P. B. Semmes, and F. Dönau, Phys. Rev. C **64**, 031304(R) (2001).
[7] T. Koike, K. Starosta, C. J. Chiara, D. B. Fossan, and D. R. LaFosse, Phys. Rev. C **63**, 061304(R) (2001).
[8] R. A. Bark, A. M. Baxter, A. P. Byrne, G. D. Dracoulis, T. Kibédi, T. R. McGoram, and S. M. Mullins, Nucl. Phys. **A691**, 577 (2001).
[9] K. Starosta, C. J. Chiara, D. B. Fossan, T. Koike, T. T. S. Kuo, D. R. LaFosse, S. G. Rohozinski, C. Droste, T. Morek, and J. Srebrny, Phys. Rev. C **65**, 044328 (2002).
[10] T. Koike, K. Starosta, C. J. Chiara, D. B. Fossan, and D. R. LaFosse, Phys. Rev. C **67**, 044319 (2003).
[11] G. Rainovski, E. S. Paul, H. J. Chantler, P. J. Nolan, D. G. Jenkins, R. Wadsworth, P. Raddon, A. Simons, D. B. Fossan, T. Koike, K. Starosta, C. Vaman, E. Farnea, A. Gadea, Th. Kröll, R. Isocrate, G. de Angelis, D. Curien, and V. I. Dimitrov, Phys. Rev. C **68**, 024318 (2003).
[12] G. Rainovski, E. S. Paul, H. J. Chantler, P. J. Nolan, D. G. Jenkins, R. Wadsworth, P. Raddon, A. Simons, D. B. Fossan, T. Koike, K. Starosta, C. Vaman, E. Farnea, A. Gadea, Th. Kröll, G. de Angelis, R. Isocrate, D. Curien, and V. I. Dimitrov, J. Phys. G **29**, 2763 (2003).
[13] S. Zhu, U. Garg, B. K. Nayak, S. S. Ghugre, N. S. Pattabiraman, D. B. Fossan, T. Koike, K. Starosta, C. Vaman, R. V. F. Janssens, R. S. Chakrawarthy, M. Whitehead, A. O. Macchiavelli, and S. Frauendorf, Phys. Rev. Lett. **91**, 132501 (2003).
[14] H. C. Jain, S. Lakshmi, and P. K. Joshi, AIP Conf. Proc. No. 764 (AIP, Melville, NY, 2005), p. 99.
[15] J. Srebrny, E. Grodner, T. Morek, I. Zalewska, Ch. Droste, J. Mierzejewski, A. A. Pasternak, J. Kownacki, and J. Perkowski, Acta Phys. Pol. B **36**, 1063 (2005).
[16] E. Grodner, J. Srebrny, A. A. Pasternak, I. Zalewska, T. Morek, Ch. Droste, J. Mierzejewski, M. Kowalczyk, J. Kownacki, M. Kisielinski, S. G. Rohozinski, T. Koike, K. Starosta, A. Kordyasz, P. J. Napiorkowski, M. Wolinska-Cichocka, E. Ruchowska, W. Plociennik, and J. Perkowski, Phys. Rev. Lett. **97**, 172501 (2006).
[17] C. Vaman, D. B. Fossan, T. Koike, K. Starosta, I. Y. Lee, and A. O. Macchiavelli, Phys. Rev. Lett. **92**, 032501 (2004).
[18] P. Joshi, D. G. Jenkins, P. M. Raddon, A. J. Simons, R. Wadsworth, A. R. Wilkinson, D. B. Fossan, T. Koike, K. Starosta, C. Vaman, J. Timár, Zs. Dombrádi, A. Krasznahorkay, J. Molnár, D. Sohler, L. Zolnai, A. Algora, E. S. Paul, G. Rainovski, A. Gizon, J. Gizon, P. Bednarczyk, D. Curien, G. Duchêne, and J. N. Scheurer, Phys. Lett. **B595**, 135 (2004).
[19] P. Joshi, A. R. Wilkinson, T. Koike, D. B. Fossan, S. Finnigan, E. S. Paul, P. M. Raddon, G. Rainovski, K. Starosta, A. J. Simons, C. Vaman, and R. Wadsworth, Eur. Phys. J. A **24**, 23 (2005).
[20] J. A. Alcántara-Núñez, J. R. B. Oliveira, E. W. Cybulska, N. H. Medina, M. N. Rao, R. V. Ribas, M. A. Rizzutto, W. A. Seale, F. Falla-Sotelo, K. T. Wiedemann, V. I. Dimitrov, and S. Frauendorf, Phys. Rev. C **69**, 024317 (2004).
[21] J. Timár, P. Joshi, K. Starosta, V. I. Dimitrov, D. B. Fossan, J. Molnár, D. Sohler, R. Wadsworth, A. Algora, P. Bednarczyk, D. Curien, Zs. Dombrádi, G. Duchene, A. Gizon, J. Gizon, D. G. Jenkins, T. Koike, A. Krasznahorkay, E. S. Paul, P. M. Raddon, G. Rainovski, J. N. Scheurer, A. J. Simons, C. Vaman, A. R. Wilkinson, L. Zolnai, and S. Frauendorf, Phys. Lett. **B598**, 178 (2004).
[22] J. Timár, C. Vaman, K. Starosta, D. B. Fossan, T. Koike, D. Sohler, I. Y. Lee, and A. O. Macchiavelli, Phys. Rev. C **73**, 011301(R) (2006).
[23] Dan Jerrestam, W. Klamra, J. Gizon, F. Liden, L. Hildingsson, J. Kownacki, Th. Lindblad, and J. Nyberg, Nucl. Phys. **A577**, 786 (1994).
[24] P. Joshi, M. P. Carpenter, D. B. Fossan, T. Koike, E. S. Paul, G. Rainovski, K. Starosta, C. Vaman, and R. Wadsworth, Phys. Rev. Lett. **98**, 102501 (2007).
[25] D. Tonev, G. de Angelis, P. Petkov, A. Dewald, S. Brant, S. Frauendorf, D. L. Balabanski, P. Pejovic, D. Bazzacco, P. Bednarczyk, F. Camera, A. Fitzler, A. Gadea, S. Lenzi, S. Lunardi, N. Marginean, O. Möller, D. R. Napoli, A. Paleni, C. M. Petrache, G. Prete, K. O. Zell, Y. H. Zhang, J.-Y. Zhang, Q. Zhong, and D. Curien, Phys. Rev. Lett. **96**, 052501 (2006).
[26] C. M. Petrache, G. B. Hagemann, I. Hamamoto, and K. Starosta, Phys. Rev. Lett. **96**, 112502 (2006).
[27] D. Jerrestam, W. Klamra, J. Gizon, B. Fogelberg, S. J. Freeman, H. J. Jensen, S. Mitarai, G. Sletten, and I. Thorslund, Nucl. Phys. **A579**, 256 (1994).
[28] K. S. Krane, R. M. Steffen, and R. M. Wheeler, Nucl. Data Tables A **11**, 351 (1973).
[29] D. C. Radford, Nucl. Instrum. Methods A **361**, 297 (1995).
[30] D. Hippe, H.-W. Schuh, B. Heits, A. Rademacher, K. O. Zell, P. v. Brentano, J. Eberth, and E. Eube, Z. Phys. A **284**, 329 (1978).
[31] R. Popli, J. A. Grau, S. I. Popik, L. E. Samuelson, F. A. Rickey, and P. C. Simms, Phys. Rev. C **20**, 1350 (1979).
[32] A. W. B. Kalshoven, W. H. A. Hesselink, T. J. Ketel, J. Ludziejewski, L. K. Peker, J. J. van Ruyven, and H. Verheul, Nucl. Phys. **A315**, 334 (1979).
[33] H.-J. Keller, S. Frauendorf, U. Hagemann, L. Kaubler, H. Prade, and F. Stary, Nucl. Phys. **A444**, 261 (1985).
[34] D. Jerrestam, B. Fogelberg, R. A. Bark, I. G. Bearden, G. Sletten, W. Klamra, J. Cederkall, S. Mitarai, T. Shizuma, and E. Makela, Phys. Rev. C **52**, 2448 (1995).

[35] A. Y. Deo, S. B. Patel, S. K. Tandel, S. Muralithar, R. P. Singh, R. Kumar, R. K. Bhowmik, S. S. Ghugre, A. K. Singh, and V. Kumar, Amita, Phys. Rev. C **73**, 034313 (2006).
[36] R. Bengtsson and S. Frauendorf, Nucl. Phys. **A327**, 139 (1979).
[37] W. Nazarewicz, G. A. Leander, and J. Dudek, Nucl. Phys. **A467**, 437 (1987).
[38] W. Nazarewicz, R. Wyss, and A. Johnson, Nucl. Phys. **A503**, 285 (1989).
[39] R. Wyss, J. Nyberg, A. Johnson, R. Bengtsson, and W. Nazarewicz, Phys. Lett. **B215**, 211 (1988).
[40] F. Dönau and S. Frauendorf, in *Proceedings of the Conference on High Angular Momentum Properties of Nuclei, Oak Ridge*, edited by N. R. Johnson (Harwood Academic, New York, 1983), p. 143; F. Dönau, Nucl. Phys. **A471**, 469 (1987).
[41] A. M. Bizzetti-Sona, P. Blasi, M. Donvito, A. A. Stefanini, D. Bazzacco, F. Brandolini, K. Löwenich, P. Pavan, C. Rossi-Alvarez, M. De Poli, and A. M. I. Haque, Z. Phys. A **335**, 365 (1990); P. Raghavan, At. Data Nucl. Data Tables **42**, 189 (1989).
[42] T. Koike, K. Starosta, P. Joshi, G. Rainovski, J. Timár, C. Vaman, and R. Wadsworth, J. Phys. G **31**, S1741 (2005).